Amino Acids (2014) 46:2415–2426
DOI 10.1007/s00726-014-1796-x

ORIGINAL ARTICLE

A routine method for cloning, expressing and purifying Aβ(1–42) for structural NMR studies

Daniel K. Weber · Marc-Antoine Sani · John D. Gehman

Received: 22 June 2014 / Accepted: 25 June 2014 / Published online: 16 July 2014

Abstract Nuclear magnetic resonance (NMR) is a key technology in the biophysicist's toolbox for gaining atomic-level insight into structure and dynamics of biomolecules. Investigation of the amyloid-β peptide (Aβ) of Alzheimer's disease is one area where NMR has proven useful, and holds even more potential. A barrier to realizing this potential, however, is the expense of the isotopically enriched peptide required for most NMR work. Whereas most biomolecular NMR studies employ biosynthetic methods as a very cost-effective means to obtain isotopically enriched biomolecules, this approach has proven less than straightforward for Aβ. Furthermore, the notorious propensity of Aβ to aggregate during purification and handling reduces yields and increases the already relatively high costs of solid phase synthesis methods. Here we report our biosynthetic and purification developments that yield pure, uniformly enriched ^{15}N and $^{13}C^{15}N$ Aβ(1–42), in excess of 10 mg/L of culture media. The final HPLC-purified product was stable for long periods, which we characterize by solution-state NMR, thioflavin T assays, circular dichroism, electrospray mass spectrometry, and dynamic light scattering. These developments should facilitate further investigations into Alzheimer's disease, and perhaps misfolding diseases in general.

Keywords Recombinant peptide · Uniform labeling · Amyloid beta peptide · Alzheimer's disease · Protein NMR · SUMO · Thioflavin T assay · Circular dichroism

D. K. Weber · M.-A. Sani · J. D. Gehman
School of Chemistry, Bio21 Institute, University of Melbourne, Melbourne, VIC, Australia

Present Address:
J. D. Gehman (✉)
GehmanLab, Woodend, VIC, Australia
e-mail: jgehman@gehmanlab.com

Abbreviations

Aβ	Amyloid beta peptide
APP	Amyloid precursor protein
CD	Circular dichroism
CV	Column volume
DLS	Dynamic light scattering
ESI-MS	Electrospray ionization mass spectrometry
Gdm.HCl	Guanidine hydrochloride
GFP	Green fluorescent protein
HSQC	Heteronuclear single quantum coherence
IPTG	Isopropyl β-D-1-thiogalactopyranoside
LB	Luria Broth
LC-MS	Liquid chromatography-mass spectrometry
MAP	Methionine aminopeptidase
NMR	Nuclear magnetic resonance
Ni–NTA	Nickel-nitrilotriacetic acid
PTM	Post-translational modification
ROS	Reactive oxygen species
RP-HPLC	Reverse-phase high-performance liquid chromatography
RT	Room temperature
SPPS	Solid phase peptide synthesis
SUMO	Small ubiquitin-like modifier
TB	Terrific broth
TEV	Tobacco etch virus protease
Ub	Ubiquitin
Ulp1	Ulb-specific protease 1

Introduction

Extracellular neuronal deposits predominantly composed of insoluble fibrillar structures of amyloid beta peptides are ubiquitous in Alzheimer's disease (AD) pathology. These peptides, varying from 39–43 residues in length, originate

from proteolytic processing of the amyloid precursor protein (APP) (Sisodia 1992), whereby production biased towards the highly amyloidogenic 42-residue isoform Aβ(1–42) is a significant risk factor towards the onset of AD (Selkoe 2012). Mechanistic links of Aβ peptides to neurodegenerative symptoms, however, have been challenging to identify, but are often proposed in relation to metal binding (Watt et al. 2012), catalytic roles in reactive oxygen species (ROS) generation (Butterfield and Lauderback 2002; Barnham et al. 2003, 2004) and perturbing interactions towards model lipid membranes (Weber et al. 2012; Gehman et al. 2008a; Lau et al. 2007a, b; Sciacca et al. 2012).

Structural data obtained from nuclear magnetic resonance (NMR) has helped to better understand the pathogenicity of Aβ peptides and to inform rational drug design efforts. NMR-based structural models include helical structures in membrane-mimetic solvents or micelles (Sticht et al. 1995; Coles et al. 1998; Watson et al. 1998; Crescenzi et al. 2002; Tomaselli et al. 2006), predominately unstructured monomers under aqueous conditions at low temperatures (Vivekanandan et al. 2011; Hou et al. 2004), and insoluble fibrillar structures rich in beta sheet (Lührs et al. 2005; Petkova et al. 2002, 2006; Paravastu et al. 2008; Lu et al. 2013). In addition to overcoming the limitations of X-ray diffraction imposed by the non-crystalline and highly polymorphic nature of Aβ peptides, NMR also provides additional information on dynamics, which could be used in conjunction with computational methods to better appreciate the conformational space populated by the peptide in its native, intrinsically disordered state (Sgourakis et al. 2011; Rosenman et al. 2013; Ball et al. 2013). Such studies are, however, limited to the availability of an inexpensive source of milligram quantities of peptide, uniformly or selectively labeled with NMR-useful isotopes (i.e., ^{13}C, ^{15}N, ^{2}H, ^{19}F, etc.).

The large quantities of protein needed for structural biology is typically supplied reasonably efficiently by biosynthesis in *E. coli* or other expression systems. The need for ^{15}N and ^{13}C isotopically enriched molecules in NMR involves simple refinement of the growth media to supply only ^{15}N- and/or ^{13}C-enriched metabolic precursors as the sole nitrogen and carbon sources, respectively. Biosynthetic expression of peptides, however, is not quite as straightforward, and solid phase peptide synthesis is more commonly employed to produce peptide by means of synthetic chemistry. Where just a few nuclei within a peptide are to be labelled, solid phase synthesis is still standard, albeit with increased cost owing to such specialized precursors (Mehta et al. 2013). Uniform labelling of peptide, however, quickly becomes cost prohibitive by solid phase synthesis. For the Aβ peptide, these problems are particularly acute, given the 40–42 residue length of the peptide, as well as the poor yields of pure, unmodified, and unoxidized material for which it is infamous [revised by Finder et al. (2010)].

Toward overcoming such limitations, mixed success has been reported with adapting for peptides the fusion-protein approach sometimes applied to problematic proteins. In this approach, recombinant DNA techniques are used to create a fusion protein where a well-behaved protein subunit is both affinity-tagged for purification ease and linked to a protein of interest with a peptide linker plus protease cleavage site, such as for TEV, Factor Xa, or enterokinase. While Aβ(1–40) and Aβ(1–42) free of extraneous N-terminal methionine (as is often the case for straight biosynthesis in *E. coli*) or other residues from sloppy protease cleavage has apparently been produced by this approach (Finder et al. 2010; Hortschansky et al. 2005; Long et al. 2011; Nagata-Uchiyama et al. 2007), adaptations of these methods for isotope labeling have only been comprehensively described for the less-amyloidogenic (and less disease-relevant) Aβ(1–40), either providing low (<2 mg/L of culture) or undisclosed final yields (Nagata-Uchiyama et al. 2007). This may in part be due to the typical losses in yield owing to the use of specialized minimal growth media compared to high-density media for routine biosynthetic protein production at natural isotopic abundance (Long et al. 2011).

In this study we provide a significantly improved protocol for producing entirely native, uniformly ^{15}N and ^{13}C^{15}N-labeled recombinant Aβ(1–42) at yields exceeding 10 mg/L of culture. A scheme based on a SUMO fusion partner is utilized, which has demonstrated promising results for expressing Aβ(1–42), albeit only from small-scale cultures (Satakarni and Curtis 2011). The potency, reliability and stability of SUMO protease (Ulp1) compared to traditionally used proteases, which are selective to degenerate linkers and required in prohibitive quantities, also provides significant advantages (Malakhov et al. 2004). Furthermore, we incorporate several attractive features including a modular cloning approach for flexibility in producing mutants or other isoforms of Aβ (Walsh et al. 2009), a fast and simple workflow for isolation and purification of amyloid beta from cleavage reactions (Finder et al. 2010) and a once-off preparation of SUMO protease (Lee et al. 2008) sufficient for routine preparative-scale implementation. The chemical and conformational state of the final product is evaluated by electrospray ionization mass spectrometry, solution NMR, thioflavin T assay and circular dichroism techniques.

Materials and methods

Cloning, expression and purification of SUMO-Aβ(1–42)

The Aβ(1–42) gene was synthesized by PCR according to the codon-optimized sequence and modular approach previously described by Walsh et al. (2009). Taq DNA

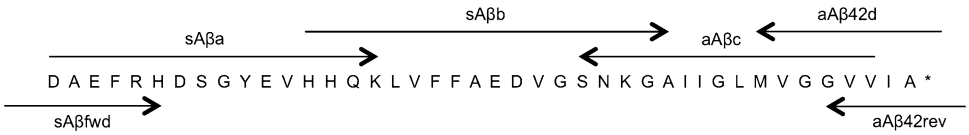

Fig. 1 PCR scheme for synthesizing the Aβ(1–42) gene. The modular approach and DNA sequence, codon-optimized for *E. coli*, was identical to that described by Walsh et al. (2009). The reaction consisted of MyTaq Red Mix, sAβa (600 nM), aAβ42d (600 nM), sAβb (40 nM) and aAβc (40 nM), and underwent 2 cycles of 94 °C (15 s) and 35 °C (45 s); 2 cycles of 94 °C (15 s), 62 °C (15 s) and 64 °C (30 s); and a further 25 cycles of 94 °C (15 s), 66 °C (15 s) and 68 °C (15 s). *Xba*I and *Bsa*I restriction sites, i.e., if T/A cloning vectors are not used, were then added by a second reaction using a one-tenth dilution of the prior reaction and primers sAβfwd (600 nM) and sAβrev (600 nM), then 2 cycles of 94 °C (15 s), 51 °C (15 s) and 52 °C (30 s); and 25 cycles of 94 °C (15 s), 66 °C (15 s) and 68 °C (15 s)

polymerase (MyTaq Red Mix, Bioline, Australia) and oligonucleotides, modified for compatibility with 3′ overhangs introduced by Taq, sAβa, 5′-GACGCTGAATTCCG TCACGACTCTGGTTACGAAGTTCACCACCAGA-3′; sAβb, 5′-CACCACCAGAAGCTGGTGTTCTTCGCT GAAGACGTGGGTTCTAACAAGGGTGCT-3′; aAβc, 5′-TTACACAACGCCACCAACCATCAGACCGATGAT AGCACCCTTGTTAGA-3′; aAβ42d, 5′-TTAAGCGATC ACAACGCCACCAACCATCAGACCGAT-3′; sAβfwd, 5′-CAGGTCTCAAGGTGACGCTGAATTCCGTCAC-3′; and aAβ42rev, 5′-CAGGTCTCTCTAGATTTAAGCGATC ACAACGCC-3′ (Micromon, Australia) were use to construct the gene (see Fig. 1) with BsaI and XbaI restriction sites for subsequent cloning into a pE-SUMOpro expression vector (T7, ampicillin; LifeSensors, Malvern, PA, USA). The construct, encoding a 6-His-tagged SUMO fused to the N-terminus of Aβ(1–42), was propagated using *E. coli* DH5α subcloning cells (Invitrogen) and verified by colony PCR and DNA sequencing (Applied Genetic Diagnostics, University of Melbourne, Australia).

For expression of unlabeled (natural abundance) SUMO-Aβ(1–42), a single colony of freshly transformed *E. coli* One Shot BL21(DE3) expression cells (Invitrogen), selected from an LB agar plate (including 100 μg/mL ampicillin), were used to inoculate LB-Miller overnight starter-cultures. Day cultures of 500 mL LB-Miller (including 100 μg/mL ampicillin) were then inoculated from 5 mL of starter-culture (OD_{600} 1.5) and grown at 37 °C with 275 RPM shaking. Cells were induced with 1 mM IPTG once the OD_{600} reached 0.6 (~3.5 h). Growth continued for 4 h (OD_{600} 1.4) before cells were harvested by centrifugation (8,000*g*, 10 min, 4 °C). Pellets were snap-frozen with N_2 (l) and stored at −20 °C (3.1 g/L culture wet cell mass).

Uniformly labeled ^{15}N and $^{13}C^{15}N$ SUMO-Aβ(1–42) were expressed from cultures grown in Neidhardt's minimal media (Neidhardt et al. 1974), with 0.52 g/L $^{15}NH_4Cl$ and 5.2 g/L [U-^{13}C]-glucose (Cambridge Isotope Laboratories) being the sole nitrogen and carbon sources, respectively. The culture media (including 100 μg/mL ampicillin) were freshly prepared using the method described by Gehman et al. (2008b), and sterile-filtered immediately prior to use. Cultures expressing ^{15}N SUMO-Aβ(1–42) were grown as described above for natural-abundance cultures and harvested 4–5 h post-induction (OD_{600} 1.1), yielding wet cell masses of 3.0 g/L of culture. For expression of $^{13}C^{15}N$ SUMO-Aβ(1–42), cells were initially grown in ^{15}N-enriched media with natural abundance glucose and centrifuged (8,000*g*, 10 min, 4 °C) once the OD_{600} reached 0.6. Pellets were resuspended in fresh $^{13}C^{15}N$-enriched media, induced at an OD_{600} 0.8, then harvested 4–5 h after induction (OD_{600} 2.1) to yield a wet cell mass of 5.5 g/L of culture.

Hexahistidine-tagged SUMO-Aβ(1–42), as reported in pilot-scale work by Satakarni and Curtis (2011), was found to accumulate in inclusion bodies when expressed in *E. coli*. Accordingly, frozen cell pellets were suspended into denaturing lysis buffer (6 M Gdm.HCl, 100 mM sodium phosphate, 10 mM tris, pH 8.0; 10 mL per 1 g wet cell mass) and sonified on ice to aid lysis (Branson 250; 50 % duty cycle, level 5 output). The crude lysate was stirred on ice for 1 h then clarified by centrifugation (10,000*g*, 30 min, RT). The supernatant was applied to a Ni–NTA agarose resin (Qiagen; 10 mL bed volume per 1.3 g of wet cell mass) and then washed with 10 column volumes (CVs) of denaturing buffer (8 M urea, 100 mM sodium phosphate, 10 mM tris, pH 8.0). The fusion protein was refolded on the resin by exchange into 100 % native buffer (50 mM sodium phosphate, 300 mM NaCl, pH 8.0) over 4 CVs, increasing concentration stepwise at 25 %/CV from denaturing buffer, then washing with a further 10 CVs of 100 % native buffer. Elution took place over 4 CVs of elution buffer (50 mM sodium phosphate, 300 mM NaCl, 250 mM imidazole, pH 8.0) and the protein stored at 4 °C. All purification steps with urea were done using chilled buffers as a precaution against possible carbamylation modifications. Purities of 60–90 % were determined from SDS-PAGE. Higher purity (>90 %) could be obtained using wash buffers at pH 6.3 (denaturing) or containing 20 mM imidazole (native), but not without significant losses from premature elution of protein. Accounting for impurities, final yields

of unlabeled, ^{15}N and $^{15}N^{13}C$ SUMO-Aβ(1–42) were 96, 96 and 181 mg/L of culture, respectively, as determined by Bradford assay (Bradford 1976) using bovine serum albumin (Sigma) as a standard.

Cleavage and purification of Aβ(1–42)

SUMO-Aβ(1–42) (~100 μM), freshly eluted from Ni–NTA resin, with 2 mM DTT added, was cleaved by Ulp1 (preparation described below), at 1,000:1 substrate to enzyme molar ratio, for 1–3 days at 4 °C. Aggregation was induced by carefully lowering the pH to between 6.5 and 7.0 with 1 M HCl and subsequent incubation at 37 °C for 3 h. Aβ(1–42) was then pelleted by centrifugation (10,000*g*, 15 min, RT) and dissolved into 8 M Gdm.HCl or 70 % formic acid (~5 mg/mL peptide). Aβ(1–42) was purified by HPLC using a preparative Phenomenex Jupiter C4 column (150 × 21.2 mm, 10 μm particle size, 300 Å pore), maintained at 60 °C using a Phenomenex Thermosphere TS-430 column heater. Sample was injected at a 2 mL/min flow rate of TFA (0.1 %) and acetonitrile (10 %) over 5 min, and eluted at 10 mL/min flow using a 20–90 % linear gradient of acetonitrile over 30 min. Elution volumes were lyophilized and stored at −20 °C. Yields of lyophilized unlabeled, ^{15}N and $^{13}C^{15}N$ Aβ(1–42) were 13, 12, and 22 mg/L of culture, respectively, equating to ~40 % of the yield expected from quantities of SUMO-Aβ(1–42) purified from cell masses.

Cloning, expression and purification of SUMO protease

DNA encoding residues 403–621 of *Saccharomyces cerevisiae* Ulp1 (SUMO Protease 1), with a hexahistidine tag on both the N and C termini (Lee et al. 2008), was obtained by gene synthesis (GeneArt, Invitrogen) and codon-optimized using the GeneOptimizer tool supplied. The gene was subsequently cloned into a pET21a(+) expression vector (Novagen) using NdeI and XhoI restriction sites on the N and C-terminus, respectively, and propagated using *E. coli* DH5α subcloning cells (Invitrogen).

For expression, sequence-verified plasmid (Applied Genetic Diagnostics, University of Melbourne, Australia) was freshly transformed into *E. coli* One Shot BL21(DE3) expression cells (Invitrogen). Cells were grown in LB-Miller media (including 100 μg/mL ampicillin) at 37 °C with 275 RPM shaking. Expression was induced with 1 mM IPTG once OD_{600} reached 0.6, and growth continued for a further 4 h (OD_{600} 1.8). Cells were harvested by centrifugation (8,000*g*, 10 min, 4 °C), frozen with N_2 (l) and stored at −20 °C (5.9 g/L of culture wet cell mass).

For purification, frozen cell pellets were resuspended into native buffer (50 mM sodium phosphate, 300 mM NaCl, 10 mM imidazole, 2 mM DTT, pH 8.0) and lysed by sonification (Branson 250, 50 % duty cycle, level 5 output), on ice, with 15 cycles of 30 s bursting and 30 s cooling periods. The lysate was clarified by centrifugation (10,000*g*, 15 min, 4 °C), and the supernatant loaded onto Ni-NTA resin (Qiagen). The resin was washed with 10 CVs of native buffer containing 20 mM imidazole and eluted with 350 mM imidazole. Fractions with Ulp1 were pooled, diluted twofold with 100 % glycerol and stored at −20 °C. The product was confirmed by LC–MS (SGE ProteCol C18, 150.0 × 2.0 mm, 5 μm particle size, 120 Å pore) using a formic acid (0.1 %) flow rate of 0.25 mL/min and a linear gradient of 5–90 % MeCN over 10 min. The average mass was 27,250.24 Da (27,249.96 amu theoretical). Yields of 60 mg/L of culture were determined using a theoretical extinction coefficient at 280 nm (28,590 M^{-1} cm^{-1}).

Mass spectrometry

All mass spectrometry was done using an Agilent TOF 6220 equipped with a dual spray electrospray ionization source. Data were recorded between 100 and 3,200 *m*/*z*, in positive-ion mode with 4,000 V capillary voltage, 250 V fragmentor voltage for protein samples (or 200 V for peptide), 65 V skimmer voltage, 250 V octopole voltage, 35 psi nebulizer pressure, and 7.0 L/min N_2 drying gas flow at 325 °C. All spectra were analyzed using Agilent MassHunter Qualitative Analysis Software (Version B.05.00, Build 5.0.519.0).

NMR spectroscopy

Lyophilized recombinant Aβ(1–42), between 1 and 2 mg, was dissolved into 500 μL of 10 % NH_3 with vortexing and 5 min bath-sonication, then lyophilized. The peptide was re-dissolved into 60 μL of 50 mM NaOH and then made to 600 μL to consist of buffer (15 mM sodium phosphate, 55 mM NaCl, pH 7.4) and 10 % D_2O. The pH was carefully corrected to 7.4 (and not adjusted for pD) by addition of HCl and centrifuged (22,000*g*, 10 min, 4 °C) to remove any aggregated material. The concentration of the supernatant was checked by absorbance at 214 nm using a theoretical coefficient (Kuipers and Gruppen 2007) of 76,848 M^{-1} cm^{-1}, and the sample loaded into an ice-cold NMR tube. Sample concentrations typically varied between 200 and 600 μM.

NMR spectra were acquired using a cryoprobe-equipped Bruker 500 MHz Avance II spectrometer. Measurements were made at 5 °C, in which the sample could remain soluble for over 1 week without any visible aggregation or detectable loss in signal. Full backbone chemical shift assignments were made using ^{15}N-HSQC, HNCO and HNCACB spectra. The ^{1}H dimensions were referenced directly to trimethylsilyl propionate-d4 (TSP-d4) at

−0.12 ppm and ^{15}N and ^{13}C frequencies indirectly by their gyromagnetic ratios (Wishart et al. 1995). Spectra were processed with NMRPipe (Delaglio et al. 1995) and analyzed using CCPNmr Analysis (Vranken et al. 2005).

Thioflavin T aggregation assays

Aggregate-free NMR samples were prepared by dissolving lyophilized synthetic (WM Keck Facility, Yale University, New Haven, CT) or recombinant Aβ(1–42) into 10 % NH_3 at ~1 mg/mL with vortexing and 5 min bath-sonication. The peptide was then lyophilized and re-dissolved into 5 mM NaOH at ~100 μM then centrifuged (22,000*g*, 10 min, 4 °C) to remove any remaining aggregates. The supernatant was then checked by absorbance at 214 nm using and experimentally determined extinction coefficient of 89,665 M^{-1} cm^{-1} for synthetic peptide and a theoretical coefficient for recombinant peptide of 76,848 M^{-1} cm^{-1}, noting that synthetic preparations have been described to have impurities that lead ~20 % overestimations of concentration using theoretical coefficients (Finder et al. 2010). Stocks of Aβ(1–42) were then made to 40 μM in buffer (30 mM sodium phosphate, 100 mM NaCl, pH 7.4) and kept on ice prior to measurements.

Aggregation assays were performed using black, clear-bottom, 96-well plates (Greiner, Fluotrac 600). Wells were prepared to a total volume of 200 μL and comprised 10 μM Aβ(1–42) and 20 μM thioflavin T (ThT, Sigma-Aldrich, St Louis, MO) in buffer. Measurements were made at 37 °C using a FLUOstar Optima plate reader with 440 and 480 nm excitation and emission filters, respectively. Wells were scanned by bottom-read every 10 min with 5 s shaking prior to measurements.

Circular dichroism

Circular dichroism (CD) measurements were made using a Chirascan-Plus (Applied Photophysics) spectrometer and recorded in triplicate from 185 to 260 nm with 1 nm step size, 1 nm bandwidth, 1 s time-per-point and 0.1 mm path-length cuvettes. Temperature was incremented stepwise from 5 to 50 °C, with 5 min equilibration time prior to each scan.

Results

Cloning, expression and purification of SUMO-Aβ(1–42)

The Aβ(1–42) gene was synthesized by an adaptation of the PCR-based modular approach described by Walsh et al. (2009). The protocol required only six oligonucleotides, in which mutations, if desired, can be made by a simple substitution of oligonucleotide components. Adaptations were made to add the required BsaI and XbaI restriction sites for subsequent insertion into the commercial SUMO expression system used, and the oligonucleotide sequences modified for compatibility with the adenine overhang introduced by Taq DNA polymerase, which, theoretically, also allows direct use of expression systems based upon TA cloning.

SUMO-Aβ(1–42) was expressed from *E. coli* BL21(DE3) cells under control of the T7/lac promoter system, grown from either LB media for natural isotopic abundance, or Neidhardt's minimal media for uniform ^{15}N and ^{13}C labeling. Yields of fusion protein were high (96 mg/L of culture) regardless of culture medium, although an obvious reduction in growth rate was observed for Neidhardt's medium (Fig. 2a). Furthermore, [U-^{13}C]-glucose requirements for $^{13}C^{15}N$ SUMO-Aβ(1–42) were essentially halved by growing cell mass to mid-log phase at natural abundance carbon (with ^{15}N-enrichment), followed by resuspension and induction under fully ^{13}C- and ^{15}N-labeled growth conditions, which yielded 181 mg of fusion protein per liter of the final culture.

As prior work has determined that this particular fusion accumulates primarily into inclusion bodies (Satakarni and Curtis 2011), lysis and initial purification steps were done using denaturing buffers. SUMO-Aβ(1–42) was simply isolated by Ni–NTA affinity chromatography on the basis of an N-terminal hexahistidine tag, whereby the use chilled buffers was sufficient for averting risks of carbamylation modifications from urea degradation (Kollipara and Zahedi 2013). Furthermore, refolding of the fusion protein was achieved rapidly by on-resin exchange into native buffer, with no loss in yield, purity or cleavage efficiency compared with refolding through 3 days of dialysis (data not shown).

ESI-LCMS revealed the average mass of SUMO-Aβ(1–42) to be 16,775 Da (Fig. 2b), exactly 131 Da less than expected and corresponds to the loss of the N-terminal methionine residue, most likely from post-translational modification (PTM) by methionine aminopeptidase (MAP) (Frottin et al. 2006). Average masses for ^{15}N and $^{15}N^{13}C$ SUMO-Aβ(1–42) were measured at 16,985 and 17,691 Da, respectively. Enrichment of ^{15}N was therefore determined to be 99 %, and ^{13}C-enrichment of doubly labeled protein was 97 % based on the assumption of 99 % ^{15}N-enrichment. SDS-PAGE analysis of expressed and purified fusion protein (Fig. 2c) shows the fusion protein to migrate as multiple bands. The apparent molecular weight and intensity of these extra bands (generally greater for isotope-enriched batches) corresponds well with additional peaks at +178 and +258 Da extra mass from ESI-MS spectra (Fig. 2b) and are consistent with addition of *α-N*-6-phosphogluconoyl (+258 Da) with subsequent

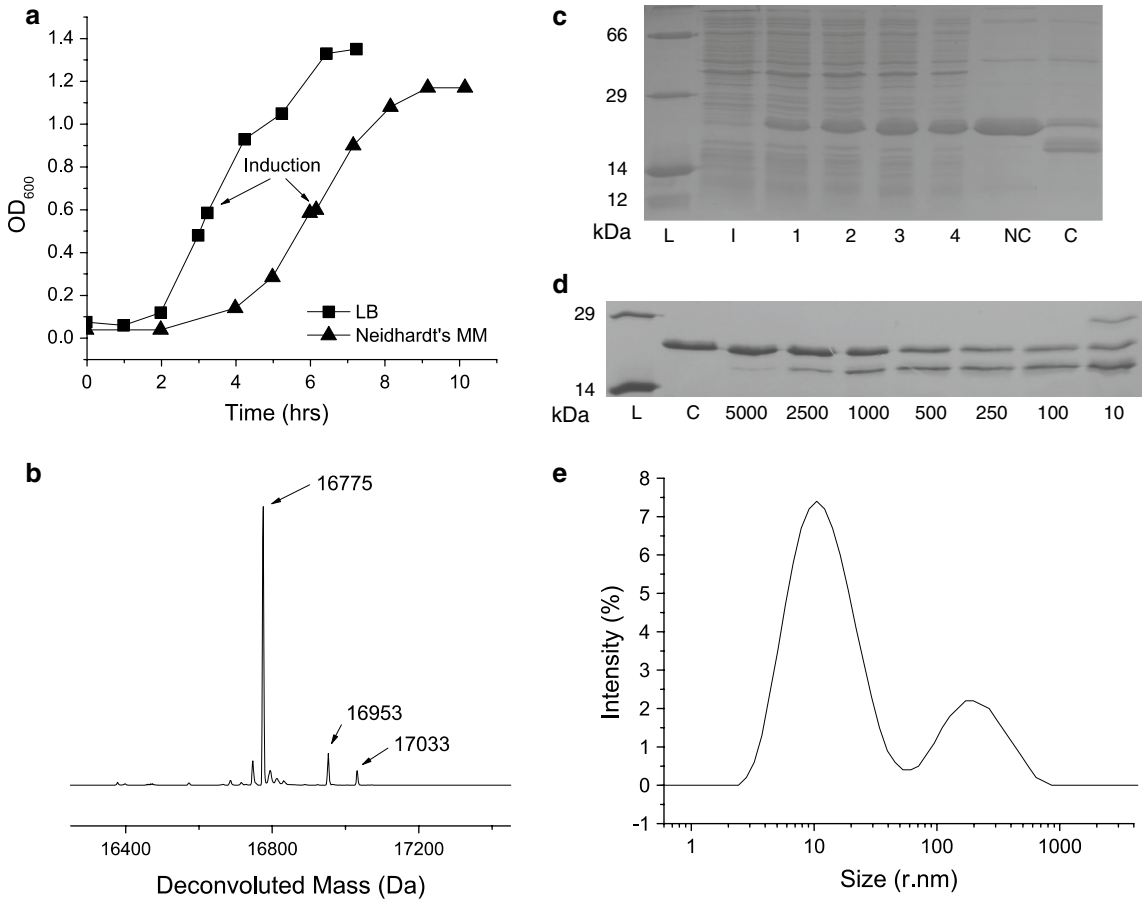

Fig. 2 **a** Growth comparison of *E. coli* cultures expressing SUMO-Aβ(1–42) from either LB media or Neidhardt's minimal media used for uniform labeling. **b** Maximum entropy deconvolution of an ESI-MS spectrum of SUMO-Aβ(1–42) at natural isotope abundance. Peaks identified at 16,953 and 17,033 likely correspond to *α-N*-gluconoyl and *α-N*-6-phosphogluconoyl PTMs, respectively. **c** 15 % SDS-PAGE gel of *E. coli* pre- and post-induction of SUMO-Aβ(1–42) expression by IPTG (hours 1–4, *lanes* 2–6); and Ni–NTA purified SUMO-Aβ(1–42), non-cleaved (NC, *lane 7*), and cleaved at 1,000:1 molar ratio of fusion protein to SUMO protease after 3 days incubation at 4 °C in native elution buffer (**c**, *lane 8*). **d** Cleavage of 10 μM SUMO-Aβ(1–42) by Ulp1 over 1 h at 4 °C in buffer (50 mM sodium phosphate, 100 mM NaCl, pH 8.0). Molar ratios of SUMO-Aβ(1–42) to protease are displayed below each lane. **e** Size-intensity distribution, proportional to the sixth power of hydrodynamic radius, from dynamic light scattering of SUMO-Aβ(1–42) in elution buffer (50 mM sodium phosphate, 300 mM NaCl, 250 mM Imidazole, pH 8.0, 4 °C). Measurements were made using a Malvern Zetasizer Nano ZS in 173° backscatter mode and analyzed by manufacturer's software

dephosphorylation to *α-N*-gluconoyl (+178 Da), which is a common N-terminal PTM for his-tagged fusion proteins (Geoghegan et al. 1999). Furthermore, the extra masses were identical between natural abundance and ^{15}N-enriched protein, as expected from being a nitrogen-free PTM, while ^{13}C-enrichment of doubly labeled material increased the observable +178 Da mass to +183 Da—roughly consistent (at least within error of mass determination) with six additional ^{13}C atoms.

Cleavage and purification of Aβ(1–42)

The active unit of SUMO protease 1 (Ulp1) is defined as the amount required to cleave 15 μg of SUMO-M-GFP at 25 °C in 1 h (Malakhov et al. 2004). Accounting for the molar mass of SUMO-Aβ(1–42), a standard reaction with 100 mg of fusion protein would require almost 15,000 units of enzyme. Enzyme requirements for routine production of Aβ(1–42) would, therefore, be cost prohibitive with current commercial sources. For this reason, we cloned and expressed a dual-his-tagged catalytic Ulp1(403-621) domain from *Saccharomyces cerevisiae* as reported by Lee et al. (2008). Expression from *E. coli* BL21(DE3) provided approximately 60 mg of enzyme per liter of culture, in which a single 1-L batch provided sufficient enzyme to cleave over 35 g of SUMO-Aβ(1–42) using the protocol described within this paper.

Cleavage of SUMO-Aβ(1–42) was performed at 4 °C to reduce risks of Aβ(1–42) aggregation throughout the reaction. Figure 2d shows that an substrate to enzyme molar ratio of 10:1 was sufficient for approximately 75 %

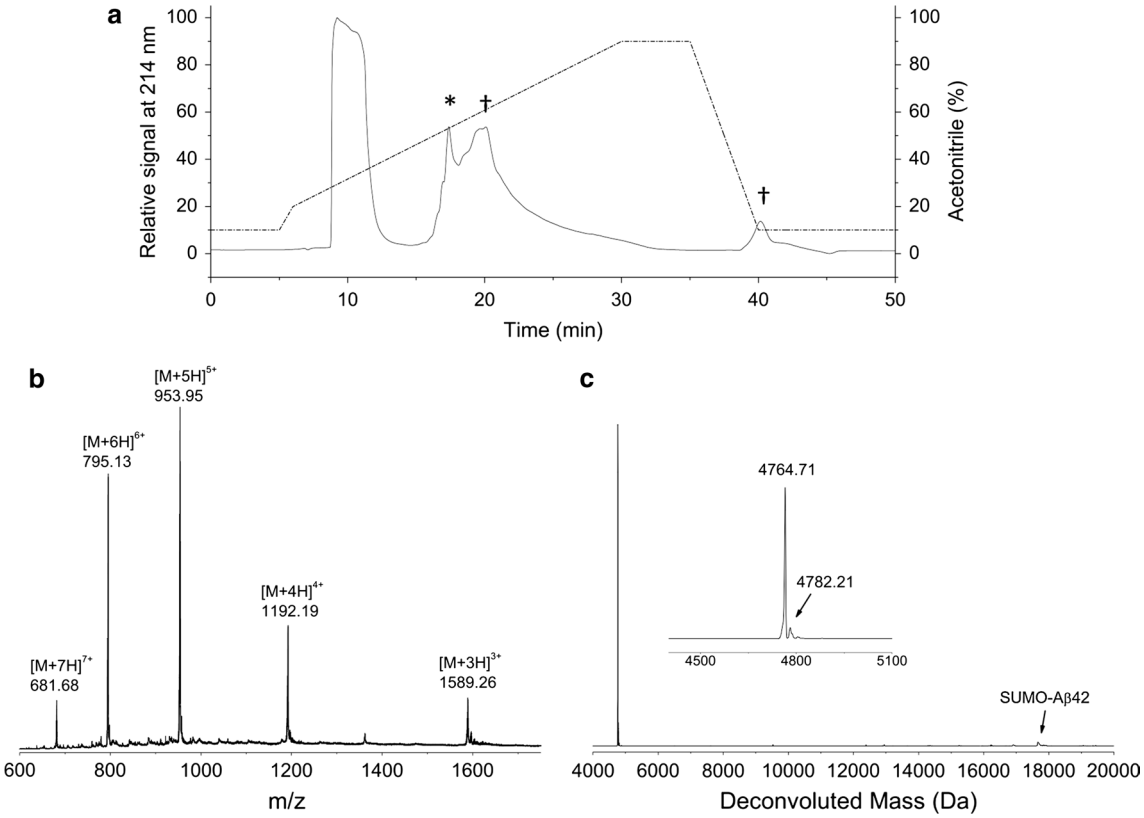

Fig. 3 **a** Preparative RP-HPLC elution profile of Aβ(1–42) detected by UV-absorbance (*solid line*) and showing acetonitrile concentration (*dashed line*). Peaks are identified corresponding to free SUMO and non-cleaved fusion protein impurities (*asterisk*) and Aβ(1–42) (*dagger*). **b** Raw and **c** maximum entropy deconvolution of ESI-MS spectrum of HPLC-purified $^{13}C^{15}N$ Aβ(1–42). A peak observed at +17.5 Da is consistent with water adducts and not oxidation of Met[35]

cleavage over 1 h at 4 °C, which is several orders of magnitude slower than previous reports of complete cleavage at ratios as low as 1:10,000 (Malakhov et al. 2004). While 4 °C is much lower than optimal range of 22–37 °C, enzyme activity was only expected to be reduced by approximately a factor of two (Malakhov et al. 2004). Soluble aggregates, however, were observed and roughly estimated by DLS to have a hydrodynamic radius of 12 nm, with intensity also centered around 200 nm arising from a small population a larger aggregates considering the sixth-power relationship of light scattering intensity to particle size (Fig. 2e). Therefore, obstruction of the cleavage site may explain the observed enzymatic inefficiencies. Nonetheless, losses in activity were compensated for by an extended cleavage duration, in which periods longer than 24 h were sufficient for maximal cleavage (~75 %) at a ratio of 1,000:1 (Fig. 2c). The tolerance of Ulp1 against high salt and imidazole content allowed cleavage to be done immediately following elution from Ni–NTA resin, i.e., without any need of buffer exchange or pH adjustment. Cleavage at ~100 μM fusion protein occurred without any visible aggregation of liberated Aβ(1–42), even upon heating to 37 °C. Subsequent pH-adjustment from 8.0 to between 6.5 and 7.0, with incubation at 37 °C for several hours, was required for complete aggregation, at which point centrifugation was convenient to purifying and concentrate Aβ(1–42) from the cleavage mixture.

Non-cleaved fusion protein co-aggregated with Aβ(1–42) and required further purification by preparative RP-HPLC to remove. SUMO-Aβ(1–42) and traces of free SUMO eluted between 15 and 18 min, while Aβ(1–42) eluted with a broad profile peaking at 20 min (Fig. 3a). The broad elution profile of Aβ(1–42) is consistent with aggregation on the column, which is expected from the highly hydrophobic nature of the peptide. ESI-MS confirmed the mass of unlabeled, ^{15}N- and $^{13}C^{15}N$ Aβ(1–42) to be 4,514.53, 4,568.64 and 4,764.23 Da (Fig. 3b, c), respectively, and only trace quantities of non-cleaved fusion protein remaining (Fig. 3c).

Biophysical characterization of Aβ(1–42)

Solution NMR on aqueous preparations was used to confirm the chemical and conformational purity of uniformly

labeled Aβ(1–42). At the high concentrations required, it is strictly necessary that pre-aggregated material is removed; otherwise, seeded fibrillization would lead to rapid loss in signal. Ammonia pretreatment, followed by dissolution into sodium hydroxide (Ryan et al. 2013) worked effectively for this purpose. Figure 4 displays a well-resolved HSQC spectrum of monomeric Aβ(1–42). Cross-peak positions are well-matched to previous spectra of either Aβ(1–40) or Aβ(1–42) with similar buffer composition and temperature (Hou et al. 2004; Long et al. 2011; Nagata-Uchiyama et al. 2007; Williamson et al. 2006; Yan et al. 2008; Danielsson et al. 2006; Broersen et al. 2011; Rezaei-Ghaleh et al. 2011; Ghalebani et al. 2012). In addition, samples maintained at 5 °C were stable for periods exceeding 1 week, which allowed confirmation of $^{1}H^{15}N$ HSQC assignments through a longer triple-resonance ^{15}N-edited HNCACB experiment. The absence of the His^{6} amide cross-peak in our HSQC is consistent with spectra reported by Williamson et al. (2006) for Aβ(1–40) (Williamson et al. 2006), while our peak positions for residues Val^{36}–Val^{40} display relative downfield shifts, possibly explained by greater beta-sheet propensity in the C-terminus for Aβ(1–42) (Hou et al. 2004). Resonances for Ala^{2} and Asp^{7} in HSQC spectra, overlapped with Ala^{30} and Asp^{23}, respectively, were assigned directly by reference to Williamson et al. (2006); however, it should be noted that our experiments could not confirm this as neither the HN(i)/CαCβ(i-1) or HN(i)/CαCβ(i) correlation was observed in HNCACB spectra for these residues. In other studies, absence of His^{13} and His^{14}, and deviations of Asp^{7}, Asn^{27} and Lys^{28} amide cross-peaks positions, relative to our HSQC spectra also exist (Hou et al. 2004; Long et al. 2011; Nagata-Uchiyama et al. 2007; Danielsson et al. 2006), and may possibly be explained by differences in sample preparation (i.e., our inclusion of NaCl, and strength of ammonia pretreatment). Furthermore, the Met^{35} chemical shift position suggests that Aβ(1–42) is in the reduced form (Hou et al. 2004), consistent with ESI-MS characterization (Fig. 3b, c).

Thioflavin T assays were used to characterize the aggregation kinetics of recombinant Aβ(1–42). Figure 5a displays a distinct lag phase, elongation phase and stationary phase over a 24-h incubation period at 37 °C for synthetic material, typical of Aβ aggregation (Sani et al. 2011). In contrast, recombinant peptide displayed negligible increases in ThT fluorescence, suggesting suppression of fibril formation at low concentration (10 μM). At significantly higher concentrations used for NMR (>200 μM), heating samples upwards of 5 °C caused rapid loss in signal and visible development of turbidity, which is consistent with fibrillization. Circular dichroism spectra of used NMR sample (5 days old), but stored at no higher than 5 °C and with no visible appearance of aggregation, showed evidence of some helical content based upon characteristic minima at

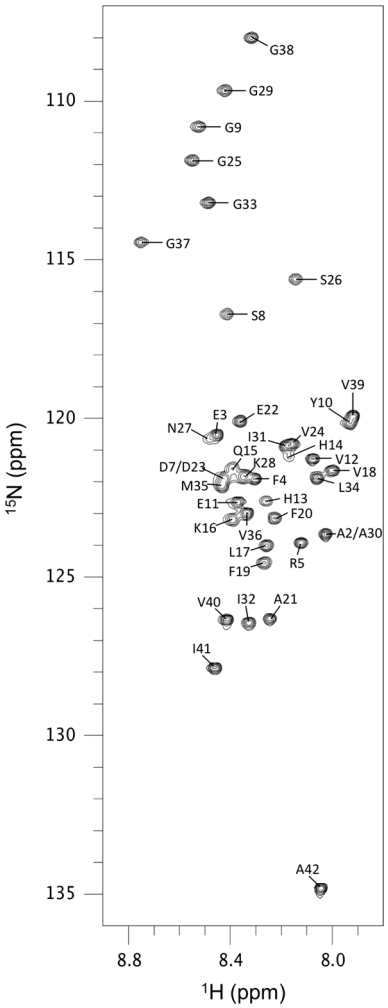

Fig. 4 500 MHz HSQC spectrum of 380 μM $^{13}C^{15}N$ Aβ(1–42) in buffer (15 mM sodium phosphate, 55 mM NaCl, pH 7.4) at 5 °C. Spectra were recorded using the standard Bruker hsqcetfpf3gpsi pulse sequence with 10.97 ppm spectral width and 2,048 points in the ^{1}H dimension, and 40 ppm spectral width and 256 points in the 15 N dimension. Processing was performed using NMRPipe (Delaglio et al. 1995) with solvent filtering, sine-bell apodization with maximum shifted to 50 % acquisition time, zero filling for both dimensions and forward-back linear prediction for the indirect ^{15}N dimension

208 and 222 nm (Fig. 5b). However, the typical lineshape produce by the presence of α-helix should lead to a ca. twofold greater positive band at 190 nm, which was not observed in Fig. 5b. The low intensity may be explained by a high proportion of random coil content producing a strong negative band at 190 nm. Upon heating from 5 to 50 °C, a two-state transition was observed with an isodichroic point at ca. 210 nm. A positive band at 195 nm and a negative band at 218 nm developed during the heating phase, typical of increasing content of β-sheet structures. This is also consistent with the NMR data where increasing the temperature induced a loss of the NMR signal due to aggregation.

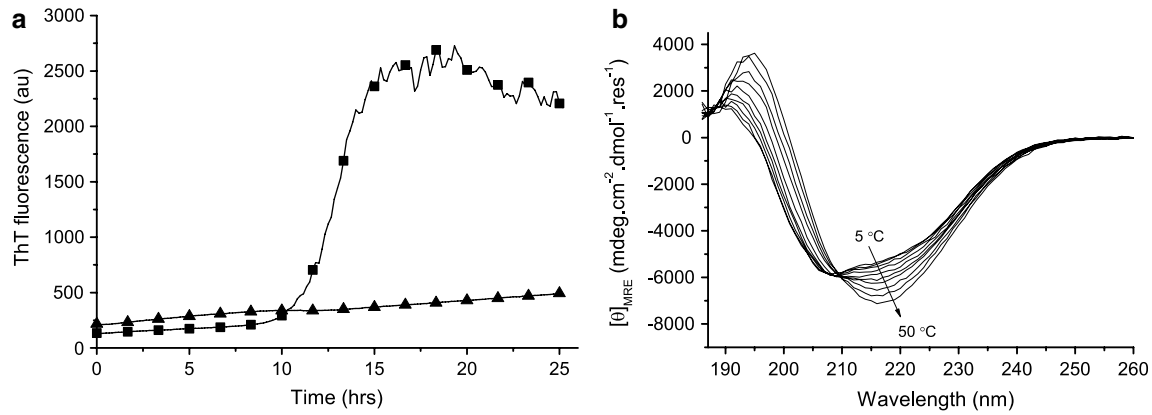

Fig. 5 **a** ThT aggregation curve of synthetic (*squares*) and recombinant (*triangles*) Aβ(1–42). Samples consisted of 10 μM peptide and 20 μM ThT in buffer (30 mM sodium phosphate, 100 mM NaCl, pH 7.4). Measurements were made at 37 °C every 10 min. **b** CD spectra of 220 μM $^{13}C^{15}N$ Aβ(1–42) after 5 days of NMR measurements at 5 °C. Temperature was incremented to 50 °C in steps of 5 °C with 5 min equilibration prior to each scan

Discussion

Here we have utilized a SUMO-Aβ(1–42) fusion for the purpose of routinely producing milligram quantities of ^{15}N and $^{13}C^{15}N$ labeled Aβ(1–42) suitable for NMR studies. Similar to other fusion strategies based on GST, HEL $(NANP)_{19}$, and MBP partners, which have previously been proven successful for expressing Aβ peptides [19–22], SUMO alleviated insolubility, could be enzymatically cleaved to release entirely native peptide (i.e., no N-Met) without any trace of N-terminal modification, and allowed single-step isolation from cell lysates, in our case from a polyhistidine tag and Ni–NTA affinity chromatography. Furthermore, SUMO does not rely upon tethering via linker sequences specific to proteases such as Factor Xa, EK or TEV, which are required in large quantities and have known instances of infidelity leading to N-terminal artifacts (Long et al. 2011; Malakhov et al. 2004). Instead, recognition intrinsic to the structure of SUMO allows SUMO protease to cleave the C-terminus with much greater fidelity and potency (Malakhov et al. 2004). For analogous advantages to SUMO, the ubiquitin (Ub)-fused Ub-Aβ(1–42) has also received interest (Lee et al. 2005) with improvements in expression and overall yields of Aβ(1–42) realized for the double-fusions GroES-Ub-Aβ(1–42) (Shahnawaz et al. 2007) and trigger factor-Ub-Aβ(1–42) (Thapa et al. 2008), but even under these improved circumstances, yields are only at comparable levels to our work despite the greater degree of complexity required.

The potential benefits of SUMO for expressing the notoriously difficult Aβ(1–42) has also been realized in past work by Satakarni and Curtis (2011), which found expression of SUMO-Aβ(1–42), extrapolated from 25 mL scale, to exceed 200 mg/L of culture. Indeed, our values (~100 mg/L of culture) were considerably lower, which may in some part be associated with the preparative (>1 L) scale of our work, our use of *E. coli* BL21(DE3) instead of an *E. coli* Rosetta (DE3) pLysS expression strain, or possibly differing methods of protein quantification [not explicitly disclosed in prior work (Satakarni and Curtis 2011)]. Furthermore, it was realized in our work that significant challenges were associated with using SUMO-Aβ(1–42) for the eventual preparative-scale production of Aβ(1–42). Firstly, despite being considerably more soluble than Aβ(1–42), the fusion construct still localizes primarily in inclusion bodies (Satakarni and Curtis 2011). While this has commonly been observed for other fusion constructs (Finder et al. 2010; Long et al. 2011; Nagata-Uchiyama et al. 2007; Shahnawaz et al. 2007), requirements for dissolution into denaturing buffers is undesirable owing to risks of protein modifications (Kollipara and Zahedi 2013) and losses in yields and time associated with refolding. Fortunately, SUMO-Aβ(1–42) could be refolded by on-resin buffer exchange, effectively averting days of dialysis. Secondly, and perhaps the most significant barrier to up-scaled application, is that even at the full published activity (Malakhov et al. 2004), a typical batch of 100 mg of SUMO-Aβ(1–42) would require ~15,000 units of enzyme to process, which by current commercial suppliers would be a cost prohibitive quantity. Furthermore, the activity of Ulp1(403-621), which we expressed by a method adapted from Lee et al. (2008), was found to be orders of magnitude less than theoretically expected (Malakhov et al. 2004); therefore, adding to already-burdensome enzyme requirements. In agreement with Satakarni and Curtis (2011), DLS analysis suggested the presence of soluble aggregates, which could have been responsible for reduced enzyme activity and ~25 % loss in overall yields of Aβ(1–42) due

Table 1 Summary of yields and ESI-MS confirmation of proteins and peptides produced from this study

	Experimental MW (Da)	Theoretical MW (Da)	Enrichment	Yield (mg/L of culture)
Ulp1	27,250.24	27,249.96	–	60
SUMO-Aβ(1–42)	16,774.73	16,775.03†	–	96
^{15}N SUMO-Aβ(1–42)	16,985.16	16,987.16†	^{15}N (99 %)	96
^{13}C^{15}N SUMO-Aβ(1–42)	17,690.91	17,717.76†	^{15}N (99 %), ^{13}C (97 %)	181‡
Aβ(1–42)	4,514.53	4,514.08	–	13
^{15}N Aβ(1–42)	4,568.64	4,568.68	^{15}N (99 %)	12
^{13}C^{15}N Aβ(1–42)	4,764.23	4,770.19	^{15}N (99 %), ^{13}C (97 %)	22‡

† Theoretical molecular weights take the loss of N-terminal methionine into account. Additional peaks at 178 Da (unlabeled, ^{15}N-labeled), 183 Da (^{13}C-labeled), and 258 Da (unlabeled, ^{15}N-labeled) may appear in ESI-MS spectra and are likely *N*-terminal α-*N*-gluconoyl and α-*N*-6-phosphogluconoyl PTMs

‡ Reported yield neglects the volume of culture used to grow cell mass under natural ^{13}C abundance

to non-cleaved fusion protein, albeit this was not an issue for the prior study. Instead, complete cleavage and activity was observed from their reactions in buffer containing 2 M urea and 37 °C, which may have destabilized aggregate assemblies to some extent, but would have also introduced risks of carbamylation modifications from urea degradation. For our work, prolonged reactions at 1,000:1 molar ratio of substrate to enzyme, at low temperature in native buffer, was an acceptable solution for reduced activity, allowing a single preparation (grown from 1 L of culture) of Ulp1(403–621) to be sufficient hundreds of preparative-scale cleavage reactions.

Overall yields of lyophilized Aβ(1–42) from our work exceeded 10 mg/L of culture at either natural isotopic abundance with uniformly ^{15}N or ^{13}C^{15}N labeling (see Table 1 for summary of yields and ESI-MS analysis). While these yields (of unlabeled peptide) could have been significantly improved by using higher-density growth media over LB (i.e., TB), doing so would have been misleading for the NMR spectroscopist given that similar yields would be unrealistic from culture media commonly used for isotope labeling—as exemplified by Long et al. in expressing a GST-Aβ40 fusion, in which a fivefold reduction in yield was observed between TB and M9 media (Long et al. 2011). In contrast, our yields of uniformly labeled material from Neidhardt's minimal media were identical to that obtained from LB.

From ESI-MS analysis, Aβ(1–42) was confirmed to be entirely free of Met^{35} oxidation or other PTMs, while solution NMR provided additional confidence that the final product obtained in a native unstructured state, and that chemical shifts were consistent with prior published work (Hou et al. 2004; Long et al. 2011; Nagata-Uchiyama et al. 2007; Williamson et al. 2006; Yan et al. 2008; Danielsson et al. 2006; Broersen et al. 2011; Rezaei-Ghaleh et al. 2011; Ghalebani et al. 2012). In addition, the peptide was remarkably stable throughout NMR acquisition, easily providing for at least 1 week of spectral acquisition despite having near-physiological concentrations of salt present, which have been noted to reduce sample lives to <24 h (Williamson et al. 2006). Furthermore, ThT assays provided further evidence that the recombinant peptide was suppressed from fibrillization relative to synthetic material, which is contrary to the conclusions made by Finder et al. that recombinant material aggregates faster as a result of being absent of the synthetic and racemic impurities inherent in SPSS (Finder et al. 2010). While the exact reasons for this discrepancy are unclear, trace quantities of non-cleaved fusion protein remaining from HPLC purification as result of broad elution profiles, evident from ESI-MS analysis, but not observable in NMR spectra, may have had some chaperoning effect. Overall, utilization of SUMO fusion methodology has proven applicable as a cost-effective means for the large-scale biosynthetic production of isotopically enriched Aβ(1–42), and possibly amyloidogenic peptides in general.

Acknowledgments The authors would like to sincerely thank Dr. Nick Williamson, Paul O'Donnell and Michael Leeming for discussions regarding ESI-MS acquisition and analysis, John Karas for advice on HPLC purification, and Professor Anthony Wedd and Dr. Zhiguang Xiao for allowing access to equipment required for cell-culture work. J. Gehman was partially funded by ARC Future Fellowship FT0991558 for this work. Circular Dichroism and Dynamic Light Scattering instruments were funded by a LIEF grant LE120100186 to G. Bryant (RMIT) and J. Gehman. D. Weber is thankful for an Australian Postgraduate Award PhD scholarship and Dowd Foundation Postgraduate Research Scholarship for Neuroscience.

Conflict of Interest The authors declare no conflict of interest.

References

Ball KA, Phillips AH, Wemmer DE, Head-Gordon T (2013) Differences in β-strand populations of monomeric Aβ40 and Aβ42. Biophys J 104:2714–2724

Barnham KJ, Ciccotosto GD, Tickler AK, Ali FE, Smith DG, Williamson NA, Lam YH, Carrington D, Tew D, Kocak G, Volitakis I, Separovic F, Barrow CJ, Wade JD, Masters CL, Cherny RA, Curtain CC, Bush AI, Cappai R (2003) Neurotoxic, redox-competent Alzheimer's β-amyloid is released from lipid membrane by methionine oxidation. J Biol Chem 278:42959–42965

Barnham KJ, Haeffner F, Ciccotosto GD, Curtain CC, Tew D, Mavros C, Beyreuther K, Carrington D, Masters CL, Cherny RA, Cappai R, Bush AI (2004) Tyrosine gated electron transfer is key to the toxic mechanism of Alzheimer's disease β-amyloid. FASEB J 18:1427–1429

Bradford MM (1976) A rapid and sensitive method for the quantitation of microgram quantities of protein utilizing the principle of protein dye binding. Anal Biochem 72:248–254

Broersen K, Jonckheere W, Rozenski J, Vandersteen A, Pauwels K, Pastore A, Rousseau F, Schymkowitz J (2011) A standardized and biocompatible preparation of aggregate-free amyloid beta peptide for biophysical and biological studies of Alzheimer's disease. Protein Eng Des Sel 24:743–750

Butterfield DA, Lauderback CM (2002) Lipid peroxidation and protein oxidation in Alzheimer's disease brain: potential causes and consequences involving amyloid β-peptide-associated free radical oxidative stress. Free Radic Biol Med 32:1050–1060

Coles M, Bicknell W, Watson RA, Fairlie DP, Craik DJ (1998) Solution structure of amyloid β-peptide(1–40) in a water-micelle environment. Is the membrane-spanning domain where we think it is? Biochemistry 37:11064–11077

Crescenzi O, Tomaselli S, Guerrini R, Salvadori S, D'Ursi AM, Temussi PA, Picone D (2002) Solution structure of the Alzheimer amyloid β-peptide (1–42) in an apolar microenvironment: similarity with a virus fusion domain. Eur J Biochem 269:5642–5648

Danielsson J, Andersson A, Jarvet J, Gräslund A (2006) 15 N relaxation study of the amyloid β-peptide: structural propensities and persistence length. Magn Reson Chem 44:S114–S121

Delaglio F, Grzesiek S, Vuister GW, Zhu G, Pfeifer J, Bax A (1995) NMRPipe: a multidimensional spectral processing system based on UNIX pipes. J Biomol NMR 6:277–293

Finder VH, Vodopivec I, Nitsch RM, Glockshuber R (2010) The recombinant amyloid-β peptide Aβ1–42 aggregates faster and is more neurotoxic than synthetic Aβ1–42. J Mol Biol 396:9–18

Frottin F, Martinez A, Peynot P, Mitra S, Holz RC, Giglione C, Meinnel T (2006) The proteomics of N-terminal methionine cleavage. Mol Cell Proteomics 5:2336–2349

Gehman JD, O'Brien CC, Shabanpoor F, Wade JD, Separovic F (2008a) Metal effects on the membrane interactions of amyloid-β peptides. Eur Biophys J 37:333–344

Gehman JD, Cocco MJ, Grindley NDF (2008b) Chemical shift mapping of γδ resolvase dimer and activated tetramer: mechanistic implications for DNA strand exchange. Biochimica et Biophysica Acta-Proteins Proteomics 1784:2086–2092

Geoghegan KF, Dixon HBF, Rosner PJ, Hoth LR, Lanzetti AJ, Borzilleri KA, Marr ES, Pezzullo LH, Martin LB, Lemotte PK, McColl AS, Kamath AV, Stroh JG (1999) Spontaneous α-N-6-phosphogluconoylation of a 'His tag' in Escherichia coli: the cause of extra mass of 258 or 178 Da in fusion proteins. Anal Biochem 267:169–184

Ghalebani L, Wahlström A, Danielsson J, Wärmländer SKTS, Gräslund A (2012) PH-dependence of the specific binding of Cu(II) and Zn(II) ions to the amyloid-β peptide. Biochem Biophys Res Commun 421:554–560

Hortschansky P, Schroeckh V, Christopeit T, Zandomeneghi G, Fändrich M (2005) The aggregation kinetics of Alzheimer's β-amyloid peptide is controlled by stochastic nucleation. Protein Sci 14:1753–1759

Hou L, Shao H, Zhang Y, Li H, Menon NK, Neuhaus EB, Brewer JM, Byeon IJL, Ray DG, Vitek MP, Iwashita T, Makula RA, Przybyla AB, Zagorski MG (2004) Solution NMR studies of the Aβ(1–40) and Aβ(1–42) peptides establish that the Met35 oxidation state affects the mechanism of amyloid formation. J Am Chem Soc 126:1992–2005

Kollipara L, Zahedi RP (2013) Protein carbamylation: in vivo modification or in vitro artefact? Proteomics 13:941–944

Kuipers BJH, Gruppen H (2007) Prediction of molar extinction coefficients of proteins and peptides using UV absorption of the constituent amino acids at 214 nm to enable quantitative reverse phase high-performance liquid chromatography-mass spectrometry analysis. J Agric Food Chem 55:5445–5451

Lau TL, Gehman JD, Wade JD, Masters CL, Barnham KJ, Separovic F (2007a) Cholesterol and clioquinol modulation of Aβ(1–42) interaction with phospholipid bilayers and metals. Biochimica et Biophysica Acta-Biomembr 1768:3135–3144

Lau TL, Gehman JD, Wade JD, Perez K, Masters CL, Barnham KJ, Separovic F (2007b) Membrane interactions and the effect of metal ions of the amyloidogenic fragment Aβ(25–35) in comparison to Aβ(1–42). Biochimica et Biophysica Acta-Biomembr 1768:2400–2408

Lee EK, Hwang JH, Shin DY, Kim DI, Yoo YJ (2005) Production of recombinant amyloid-β peptide 42 as an ubiquitin extension. Protein Expr Purif 40:183–189

Lee CD, Sun HC, Hu SM, Chiu CF, Homhuan A, Liang SM, Leng CH, Wang TF (2008) An improved SUMO fusion protein system for effective production of native proteins. Protein Sci 17:1241–1248

Long F, Cho W, Ishii Y (2011) Expression and purification of 15 N- and 13C-isotope labeled 40-residue human Alzheimer's β-amyloid peptide for NMR-based structural analysis. Protein Expr Purif 79:16–24

Lu JX, Qiang W, Yau WM, Schwieters CD, Meredith SC, Tycko R (2013) Molecular structure of β-amyloid fibrils in Alzheimer's disease brain tissue. Cell 154:1257–1268

Lührs T, Ritter C, Adrian M, Riek-Loher D, Bohrmann B, Döbeli H, Schubert D, Riek R (2005) 3D structure of Alzheimer's amyloid-β(1–42) fibrils. Proc Natl Acad Sci USA 102:17342–17347

Malakhov MP, Mattern MR, Malakhova OA, Drinker M, Weeks SD, Butt TR (2004) SUMO fusions and SUMO-specific protease for efficient expression and purification of proteins. J Struct Funct Genomics 5:75–86

Mehta AK, Rosen RF, Childers WS, Gehman JD, Walker LC, Lynn DG (2013) Context dependence of protein misfolding and structural strains in neurodegenerative diseases. Biopolymers 100:722–730

Nagata-Uchiyama M, Yaguchi M, Hirano Y, Ueda T (2007) Expression and purification of uniformly 15 N-labeled amyloid β peptide 1–40 in *Escherichia coli*. Protein Pept Lett 14:788–792

Neidhardt FC, Bloch PL, Smith DF (1974) Culture medium for enterobacteria. J Bacteriol 119:736–747

Paravastu AK, Leapman RD, Yau WM, Tycko R (2008) Molecular structural basis for polymorphism in Alzheimer's β-amyloid fibrils. Proc Natl Acad Sci USA 105:18349–18354

Petkova AT, Ishii Y, Balbach JJ, Antzutkin ON, Leapman RD, Delaglio F, Tycko R (2002) A structural model for Alzheimer's β-amyloid fibrils based on experimental constraints from solid state NMR. Proc Natl Acad Sci USA 99:16742–16747

Petkova AT, Yau WM, Tycko R (2006) Experimental constraints on quaternary structure in Alzheimer's β-amyloid fibrils. Biochemistry 45:498–512

Rezaei-Ghaleh N, Andreetto E, Yan LM, Kapurniotu A, Zweckstetter M (2011) Interaction between amyloid beta peptide and an aggregation blocker peptide mimicking islet amyloid polypeptide. PLoS One 6:e20289

Rosenman DJ, Connors CR, Chen W, Wang C, García AE (2013) Aβ monomers transiently sample oligomer and fibril-like

configurations: ensemble characterization using a combined MD/NMR approach. J Mol Biol 425:3338–3359

Ryan TM, Caine J, Mertens HDT, Kirby N, Nigro J, Breheney K, Waddington LJ, Streltsov VA, Curtain C, Masters CL, Roberts BR (2013) Ammonium hydroxide treatment of Aβ produces an aggregate free solution suitable for biophysical and cell culture characterization. Peer J 1:e73

Sani MA, Gehman JD, Separovic F (2011) Lipid matrix plays a role in Abeta fibril kinetics and morphology. FEBS Lett 585:749–754

Satakarni M, Curtis R (2011) Production of recombinant peptides as fusions with SUMO. Protein Expr Purif 78:113–119

Sciacca MFM, Kotler SA, Brender JR, Chen J, Lee DK, Ramamoorthy A (2012) Two-step mechanism of membrane disruption by Aβ through membrane fragmentation and pore formation. Biophys J 103:702–710

Selkoe DJ (2012) Preventing Alzheimer's disease. Science 337:1488–1492

Sgourakis NG, Merced-Serrano M, Boutsidis C, Drineas P, Du Z, Wang C, Garcia AE (2011) Atomic-level characterization of the ensemble of the Aβ(1–42) monomer in water using unbiased molecular dynamics simulations and spectral algorithms. J Mol Biol 405:570–583

Shahnawaz M, Thapa A, Park IS (2007) Stable activity of a deubiquitylating enzyme (Usp2-cc) in the presence of high concentrations of urea and its application to purify aggregation-prone peptides. Biochem Biophys Res Commun 359:801–805

Sisodia SS (1992) β-Amyloid precursor protein cleavage by a membrane-bound protease. Proc Natl Acad Sci USA 89:6075–6079

Sticht H, Bayer P, Willbold D, Dames S, Hilbich C, Beyreuther K, Frank RW, Rosch P (1995) Structure of amyloid A4-(1–40)-peptide of Alzheimer's disease. Eur J Biochem 233:293–298

Thapa A, Shahnawaz M, Karki P, Dahal GR, Sharoar MG, Shin SY, Lee JS, Cho B, Park IS (2008) Purification of inclusion body-forming peptides and proteins in soluble form by fusion to Escherichia coli thermostable proteins. Biotechniques 44:787–796

Tomaselli S, Esposito V, Vangone P, Van Nuland NAJ, Bonvin AMJJ, Guerrini R, Tancredi T, Temussi PA, Picone D (2006) The α-to-β conformational transition of Alzheimer's Aβ-(1–42) peptide in aqueous media is reversible: a step by step conformational analysis suggests the location of β conformation seeding. Chem Bio Chem 7:257–267

Vivekanandan S, Brender JR, Lee SY, Ramamoorthy A (2011) A partially folded structure of amyloid-beta(1–40) in an aqueous environment. Biochem Biophys Res Commun 411:312–316

Vranken WF, Boucher W, Stevens TJ, Fogh RH, Pajon A, Llinas M, Ulrich EL, Markley JL, Ionides J, Laue ED (2005) The CCPN data model for NMR spectroscopy: development of a software pipeline. Proteins: Structure. Funct Genet 59:687–696

Walsh DM, Thulin E, Minogue AM, Gustavsson N, Pang E, Teplow DB, Linse S (2009) A facile method for expression and purification of the Alzheimer's disease-associated amyloid β-peptide. FEBS J 276:1266–1281

Watson AA, Fairlie DP, Craik DJ (1998) Solution structure of methionine-oxidized amyloid β-peptide (1–40). Does oxidation affect conformational switching? Biochemistry 37:12700–12706

Watt AD, Villemagne VL, Barnham KJ (2012) Metals, membranes, and amyloid-β oligomers: key pieces in the Alzheimer's disease puzzle? In: Perry G, Zhu X, Smith MA, Sorensen A, Avila J (eds), 3rd edn. 33:S283–S293

Weber DK, Gehman JD, Separovic F, Sani MA (2012) Copper modulation of amyloid beta 42 interactions with model membranes. Aust J Chem 65:472–479

Williamson MP, Suzuki Y, Bourne NT, Asakura T (2006) Binding of amyloid β-peptide to ganglioside micelles is dependent on histidine-13. Biochem J 397:483–490

Wishart DS, Bigam CG, Yao J, Abildgaard F, Dyson HJ, Oldfield E, Markley JL, Sykes BD (1995) 1H, 13C and 15 N chemical shift referencing in biomolecular NMR. J Biomol NMR 6:135–140

Yan Y, McCallum SA, Wang C (2008) M35 oxidation induces Aβ40-like structural and dynamical changes in Aβ42. J Am Chem Soc 130:5394–5395